

The spatial relationship of air temperature and land surface temperature under the different climatic types in the Philippines from 2005 to 2019

JUAN PAOLO A. ALCALDE, ADA KOREEN V. BACAY, RHAYLEN KEA C. SITOY, and DAVID BRYAN C. LAO

Philippine Science High School Western Visayas Campus - Department of Science and Technology (DOST-PSHS WVC), Brgy. Bito-on, Jaro, Iloilo City 5000, Philippines

Article Info

Submitted: July 15, 2022
Approved: Sept 23, 2022
Published: Oct 10, 2022

Keywords:

land surface temperature
air temperature
relationship
Philippines
climate types

Abstract

The urban heat island (UHI) effect is characterized by the accumulation of heat due to anthropological activities. Land surface temperature (LST) and air temperature (T_{air}) are key parameters in quantifying UHI, and they are generally believed to be well-coupled. However, these two variables respond differently to various factors, such as solar insolation, atmospheric condition, and land surface properties. Climate is a critical factor that affects LST- T_{air} relationship. Thus, this study assessed the relationship between LST and T_{air} across the different climatic types in the Philippines from 2005 to 2019. The obtained LST- T_{air} relationship coefficients for the daytime observations are 0.68, 0.47, 0.59, and 0.53 for Types I, II, III, and IV, respectively. For the nighttime observations, the obtained LST- T_{air} relationship coefficients for Types I, II, III, and IV are 0.81, 0.39, 0.66, and 0.59, respectively. Thus, for both daytime and nighttime observations, the coefficient of LST and T_{air} relationship follows a decreasing trend as areas approach the east. This implies that climatic properties such as rainfall, Northeast monsoon, and trade winds might have affected their relationship because of the sensitivity and variability in the response of LST to these factors relative to T_{air} .

Introduction. - In light of climate change, it is essential to have structured research on the relationship between urban heat islands and their climatic factors. UHI occurs when cities replace the natural land cover with dense concentrations of pavement, buildings, and other surfaces that absorb and retain heat. Due to surface modifications that are attributable to urbanization, there is a tendency for urban areas to feel crucially warmer and exhibit elevated temperatures compared to non-urbanized and rural areas [1]. The surface materials' internal properties, including thermal inertia, conductivity, and heat capacity, are the major factors that affect how the temperature of the materials varies with respect to their surroundings [2]. LST and T_{air} are used to quantify urban heat islands [3]. Due to the urban heat island phenomenon's effects on the environment, climate, and public health, it has attracted the public's attention and various researchers [4].

Studies on LST with respect to different factors such as land cover, surface albedo, and many more have long existed. For example, Ibrahim [2] has already studied the effect of land use/land cover change on LST. However, Ali et al. [5] suggested that other factors influencing LST, such as meteorological conditions, surface energy parameters, and geometrical factors, should be investigated because the relationship of LST to these has not been fully understood. As for meteorological conditions, Tomlinson et al. [5] and Nichol et al. [7] stated that

there still exists a significant gap in LST research, which is the quantification of the relationship between measured T_{air} and remotely sensed LST data. Studies assessing the relationship between T_{air} and LST found that they are correlated and that the relationship is affected by land cover, elevation, seasonality, and location [4, 7, 8]. Though these studies have investigated the LST- T_{air} relationship, there are still conditions and other parameters that are not considered. Cao et al. [4] stated that local climate zones would provide a better understanding of the variations in spatiotemporal patterns of T_{air} and suggested that future studies should be made on cities of different sizes and under different climates.

Thus, this study assessed the spatial relationship of T_{air} and LST under the different climatic types (Type I to IV) of the modified Corona's climate classification, as recognized by PAGASA, in the Philippines from 2005 to 2019. They are characterized by oppressive humidity, plenty of rainfall, and a relatively high temperature [10]. Areas under Type I have two pronounced seasons: wet and dry. For Type II, there is no dry season with very pronounced rainfall. Seasons are not very pronounced in areas under Type III. For areas under the Type IV climate, rainfall is evenly distributed throughout the year [10].

This study provides an additional description of the relationship dynamics between LST and T_{air} since it is assessed under the different climate types in the Philippines. Moreover, to address the problem

How to cite this article:

CSE: Alcalde JP, Bacay AK, Sitoy RK. 2021. The spatial relationship of air temperature and land surface temperature under the different climatic types in the Philippines from 2005 to 2019. *Publiscience*. 5(1): 50–55.

APA: Alcalde, J.P., Bacay, A.K., & Sitoy, R.K. (2021). The spatial relationship of air temperature and land surface temperature under the different climatic types in the Philippines from 2005 to 2019. *Publiscience*, 5(1), 50–55.

For supplementary data, contact: publiscience@wvc.pshs.edu.ph.



of missing data, future studies can use this research paper to develop a model to estimate the LST using the situ T_{air} , or vice versa. Specifically, this study aims:

- (i) To determine the 8-day average daytime and nighttime land surface temperature (LST_{day} and LST_{night}) from 2005-2019 for each weather station of each climate type from the raw data acquired from the Moderate Resolution Imaging Spectroradiometer (MODIS) of the National Aeronautics and Space Administration's (NASA) Earthdata;
- (ii) To determine the 8-day average minimum and maximum air temperature (T_{max} and T_{min}) from 2005 to 2019 from the daily raw data acquired from the Philippine Atmospheric, Geophysical, and Astronomical Services Administration (PAGASA);
- (iii) To impute the missing daily T_{air} data and 8-day average LST data in all places with a weather station from 2005 to 2019 using the multiple imputation method;
- (iv) To calculate Pearson's correlation coefficient between LST_{day} and T_{max} , and LST_{night} and T_{min} in all weather stations for each climate type;
- (v) To generate graphs for the pairings of LST_{day} and T_{max} , and LST_{night} and T_{min} for each climate type; and
- (vi) To examine the relationship between LST_{day} and T_{max} , and LST_{night} and T_{min} in all weather stations for each climate type using Pearson's correlation coefficient analysis and graphical analysis.

Methods. - The data gathering procedure was divided into three parts: (1) acquisition of T_{air} and LST from PAGASA and NASA's Earth Science Data Systems (ESDS) Program, respectively, from 2005 to 2019 (2) the aggregation of T_{air} data into 8-day averages, and (3) imputation of missing values.

Study Area. The study area includes all locations in the Philippines with available PAGASA weather stations for the accessible acquisition of the raw data on T_{air} .

For Type I, the weather stations are: Ambulong, Batangas; San Jose, Occidental Mindoro; Sangley Pt., Cavite; Science Garden, Quezon City; Sinit, Ilocos Sur; NAIA, Pasay City; Port Area, Manila; Laoag City, Ilocos Sur; Iba, Zambales; Subic Bay, Olongapo; Cuyo, Palawan; Dagupan City, Pangasinan; Clark Airport, Pampanga; Coron, Palawan; Baguio City, Benguet; and Cabanatuan, Nueva Ecija.

Type II: Alabat Quezon; Virac, Catanduanes, Surigao, Surigao Del Norte; Guiuan, Eastern Samar; Hinatuan, Surigao Del Sur; Infanta, Quezon; Juban, Sorsogon; Daet, Camarines Norte; Calayan, Cagayan; Casiguran, Aurora; Catarman, Northern Samar; Baler, Aurora; Borongan, Eastern Samar.

Type III: Aparri, Cagayan; Tayabas, Quezon; Tuguegarao, Cagayan; Zamboanga, Zamboanga Del Sur; Tanay, Rizal; Puerto Princesa, Palawan;

Romblon; Roxas City, Capiz; Masbate; Mactan International Airport, Cebu; Dumaguete, Negros Oriental; El Salvador City, Misamis Oriental; Capalan, Oriental Mindoro; Cotabato City, Maguindanao.

Type IV: Tacloban City, Leyte; Legaspi City, Albay; Maasin, Southern Leyte; Malaybalay, Bukidnon; Itbayat, Batanes; Dausi, Bohol; Davao City, Davao Del Sur; Dipolog, Zamboanga Del Norte; General Santos, Cotabato; Basco, Batanes; Butuan City, Agusan Del Norte; Catbalogan, Western Samar.

Acquisition of T_{air} and LST. A request for the daily T_{max} and T_{min} was made on the Philippines' Freedom of Information website. Then, LST_{day} and LST_{night} with a temporal resolution of 8-days were acquired from MODIS Aqua land product of NASA's ESDS program. Additionally, PAGASA can only provide T_{air} data from 2019 at the latest. To accurately represent climate as a parameter, fifteen years of recent data must be utilized, as stated by the National Oceanic and Atmospheric Administration [11]. Taking this into consideration, the requests were made for all weather stations from January 1, 2005 to December 31, 2019. Then, locations with more than 50% missing data were removed from the population.

Data Aggregation. The LST and T_{air} data of all selected areas from 2005 to 2019 was processed to match the temporal resolution of the 8-day averages. This was computed and tabulated using a spreadsheet.

Imputation. The imputation of data was done using the R software version 4.1.1 in RStudio v2021.09.2+382.pro1. Multiple imputation creates valid statistical inference, it is strong against outliers, and it can deal with skewed distributions and multicollinearity. The degree of absence was first determined using Little's missing completely at random (MCAR) test. Then, multiple imputation using the imputation by classification and regression trees in the multivariate imputation by chained equations (MICE) package was done for MCAR data [12]. For missing not at random (MNAR) data, imputation by random forests in MICE was used [13].

Data Analysis. The T_{air} was subtracted from the LST to calculate the mean difference in every climate type. A positive mean difference indicates that LST is greater than T_{air} . When T_{air} is greater than LST, the mean difference is negative.

To create a graph, the T_{air} and LST were plotted for each observed climatic type during the day and night. Each point represents the 8-day average LST and T_{air} data, with LST as the x-axis and T_{air} as the y-axis. For the daytime graph, T_{max} was paired with LST_{day} . For the nighttime graph, T_{min} was paired with LST_{night} .

Then, Pearson's correlation coefficient analysis was performed using the R Statistical Package software. The relationship between T_{air} and LST data for each climatic condition during the day and night was then analyzed. The magnitude and direction of the correlation were determined using the Pearson's correlation coefficient analysis guide set by Schober et al.

[12] and Cohen [13].

Results and Discussion. - The results and discussion section is divided into five parts: (1) LST- T_{air} Mean Difference, (2) the Comparison of the Obtained Pearson's Correlation Coefficient to Other Studies, (3) Linearity and Direction of the Relationship, (4) LST- T_{air} Relationship Trends, and (5) Limitations.

LST- T_{air} Mean Difference. A positive value was found for Types I and III during the day, while the mean difference was negative for Types II and IV. This indicates that for Types I and III, LST_{day} is higher than T_{max} . For Types II and IV, LST_{day} is lower than T_{max} .

Table 1. Mean difference of LST_{day} and T_{max} .

| Climate Type | Mean LST_{day} (°C) | Mean T_{max} (°C) | Daytime Mean Difference (°C) |
|--------------|-----------------------|---------------------|------------------------------|
| Type I | 37 ± 6 | 31 ± 3 | 6 ± 4 |
| Type II | 29 ± 3 | 31 ± 2 | -2 ± 3 |
| Type III | 31 ± 4 | 31 ± 2 | 0.4 ± 4 |
| Type IV | 30 ± 4 | 31 ± 2 | -0.3 ± 4 |

It was found that in climate Types I and III, the mean LST_{day} is higher than the T_{max} . LST_{day} tends to be higher than T_{max} over the dry tropics because the clear-sky insolation in these areas is high enough to elevate LST_{day} [8]. Moreover, Shen and Leptoukh [14] found that radiative forcing, which is the measure of the imbalance of the Earth's energy budget, due to the low thermal capacity, inertia, and conductivity is prominent in dry regions because of their lack of soil water. Additionally, Pullen et al. [16] found that the monthly mean rainfall in the Philippines has a pronounced east to west gradient. This means that the western part of the Philippines receives a lower amount of rainfall. Areas under Types I and III are located in the western portion of the Philippines. Thus, these areas are considered to be dry regions due to lack of rainfall. In a similar study, Good et al. [7] also discovered that LST_{day} tends to be warmer than T_{max} over the dry tropics in all seasons.

On the other hand, LST_{day} is found to be lower than T_{max} in climates Types II and IV. Since these areas are located near the Pacific Ocean, the water vapor coming from the sea warms T_{max} through latent heat fluxes [17]. Additionally, areas under Types II and IV climates are located in the eastern part of the Philippines, thus receiving a higher amount of rainfall [17]. These areas are less sensitive to radiative forcing due to their lower heat capacity and higher thermal inertia [18]. Moreover, Guha and Govill [19] demonstrated that vegetation seasonality is a direct consequence of rainfall. So, through evapotranspiration, vegetation can pump soil water into the atmosphere, remove a large amount of land surface energy, and facilitate cloud formation, which can then reduce the amount of sunlight that reaches the surface of the Earth [20, 21, 22, 23]. They also have larger aerodynamic surface roughness which

triggers strong turbulence. This allows them to transfer energy and mass from the land surface to the atmosphere more effectively [20, 21]. As a result, T_{max} becomes warmer than LST_{day} in regions with consistent rainfall in Types II and IV climate types.

For the nighttime observation, a negative mean difference was found during the night for all climate types, which implies that LST_{night} is lower than T_{min} .

Table 2. Mean difference of LST_{night} and T_{min} .

| Climate Type | Mean LST_{night} (°C) | Mean T_{min} (°C) | Nighttime Mean Difference (°C) |
|--------------|-------------------------|---------------------|--------------------------------|
| Type I | 22 ± 3 | 23 ± 3 | -1 ± 2 |
| Type II | 22 ± 2 | 24 ± 1 | -2 ± 2 |
| Type III | 22 ± 5 | 24 ± 2 | -2 ± 2 |
| Type IV | 22 ± 3 | 23 ± 2 | -1 ± 2 |

The variation in the $LST_{night}-T_{min}$ difference variation is mostly affected by emissivity properties of the surface, relative humidity, and wind speed [24]. During the night, there is a rapid elevation of T_{min} relative to LST_{night} because nighttime T_{min} is inherently more sensitive to climate forcing and perturbations to the radiation balance. The boundary layer of air is at its thinnest state. Because of this, there is less air to be warmed, and the built-up greenhouse gasses cause its extra energy to be added to the climate system [25]. The heat transfer at night is also characterized by radiative cooling of the ground and formation of an inversion layer, heating T_{min} more than LST_{night} [26]. Thus, these factors result in a rapid elevation of T_{min} relative to LST_{night} during the night.

Comparison of the Obtained Pearson's Correlation Coefficient to Other Studies. Presented in Tables 3 and 4 are the values and interpretations of daytime and nighttime Pearson's correlation coefficient, respectively.

Table 3. Value and interpretation of Pearson's correlation coefficient for the daytime graph.

| Location | R | Interpretation | p-value (10^{-17}) |
|----------|------|-----------------------------------|------------------------|
| Type I | 0.68 | Positive and Moderate Correlation | 22 |
| Type II | 0.47 | Positive and Moderate Correlation | 22 |
| Type III | 0.59 | Positive and Moderate Correlation | 22 |
| Type IV | 0.53 | Positive and Moderate Correlation | 22 |

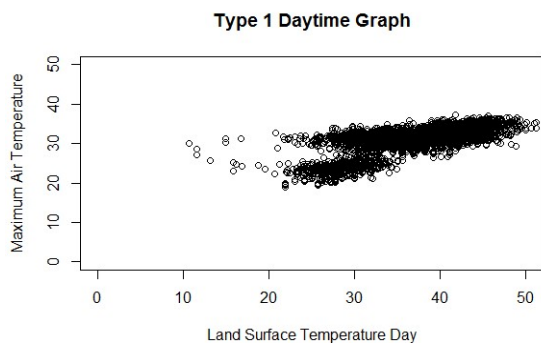
Table 4. Value and interpretation of Pearson's correlation coefficient for the nighttime graph.

| Location | R | Interpretation | p-value (10^{-17}) |
|----------|------|-----------------------------------|------------------------|
| Type I | 0.81 | Positive and Strong Correlation | 22 |
| Type II | 0.39 | Positive and Weak Correlation | 22 |
| Type III | 0.66 | Positive and Moderate Correlation | 22 |
| Type IV | 0.59 | Positive and Moderate Correlation | 22 |

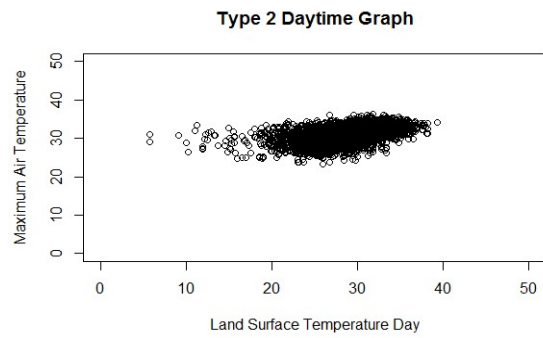
For both the pairings of LST and T_{air} , this study discovered that the two variable's correlation value is relatively lower, with the highest Pearson's correlation coefficient being 0.81 in the Type I climate during the night, as compared to studies done at areas with higher latitude. For instance, in Alaska, the obtained correlation coefficients are above 0.9 [26]. This finding is supported by Good et al. [7] as they found that the slope and correlation over the regions surrounding the equator are shown to be substantially lower. Mildrexler [27] found that the LST- T_{air} relationship often weakens as temperature increases. This is true for areas near the equator as they experience the most solar insolation throughout the year as they receive direct parallel rays from the sun and the rays concentrate on a smaller surface area, which easily heats up the region [28].

Linearity and Direction of the Relationship. Based on the result of the correlation coefficient and graphical interpretations, there is a significant linear relationship between LST and T_{air} , both for daytime and nighttime analysis in all climate types. By analyzing the Pearson's correlation coefficients and graphs in Figures 1 and 2, it was also found that the LST and T_{air} relationship is positive.

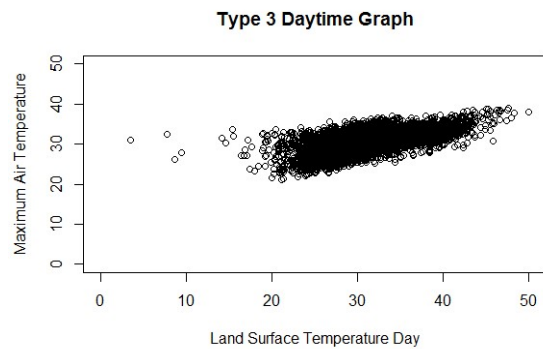
relationship is positive.



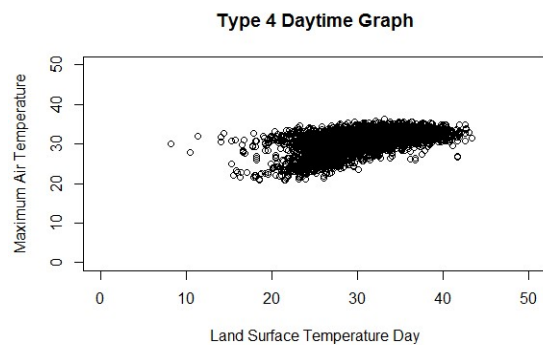
(a)



(b)

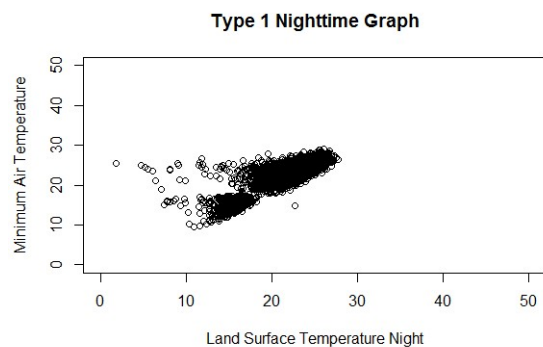


(c)



(d)

Figure 1. Plotted daytime LST vs T_{air} graphs of (a) Type I, (b) Type II, (c) Type III, and (d) Type IV climates. Error bars are omitted.



(a)

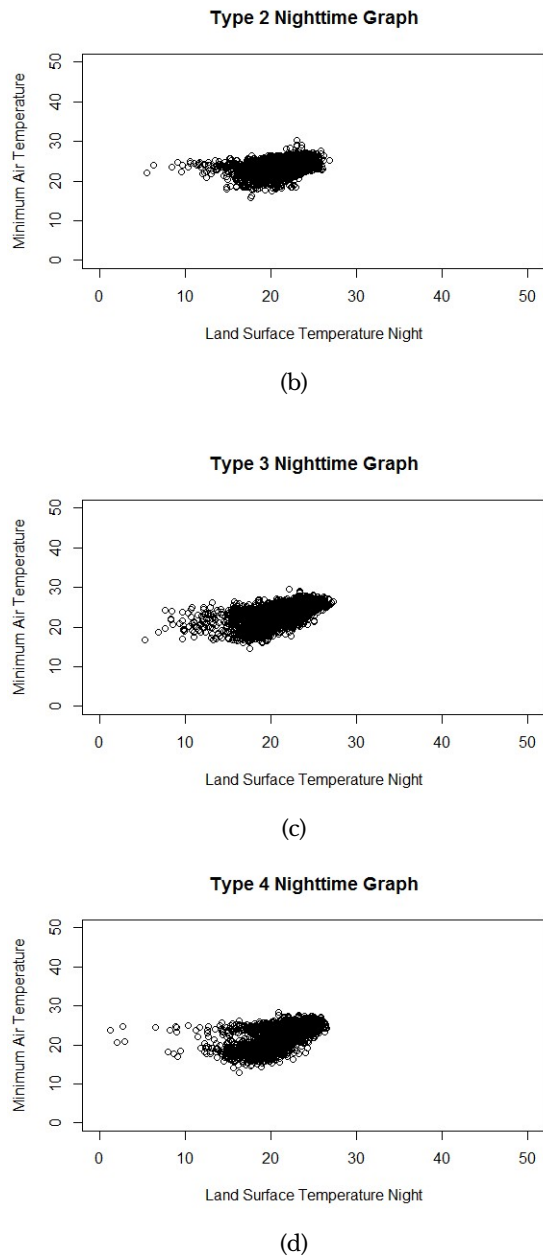


Figure 2. Plotted nighttime LST vs T_{air} graphs of (a) Type I, (b) Type II, (c) Type III, and (d) Type IV climates. Error bars are omitted.

LST and T_{air} are positively and linearly correlated due to the heat exchange between the surface and the atmosphere [29]. This heat transfer process is strongly influenced by the radiation budget and atmospheric contributions. Most of the radiation given by the sun is absorbed by the Earth's surface, therefore warming it. Then, infrared radiation is emitted by the surface, thus initiating convection cells in the atmosphere [30]. Though many factors such as topography, seasonality, and other climatic properties affect their relationship, they are still interpreted to be linear. This finding is consistent with all related studies such as that of Mutiibwa et al. [24] and Colombi et al. [31], among many others. Mutiibwa et al. [24] stated that the linear relationship can be used to create simple linear

models. With this, LST can be used as a predictor of T_{air} and vice versa. Moreover, Colombi et al. [31] made use of the linear relationship between LST and T_{air} to develop a model. It proved the validity of LST as a parameter to calculate the daily air temperature.

LST- T_{air} Relationship Trends. During the day, all the climate types exhibited a moderate correlation. During the night, Type I and III have a strong LST- T_{air} correlation while Type IV has a moderate correlation and Type II has a weak correlation. However, from both observations, a trend in their specific Pearson's correlation value can be observed. The relationship weakens as the areas approach the Pacific ocean.

Areas under Types II and IV are along or near the eastern coast which makes them susceptible to the Northeast monsoon, trade winds, and cyclonic storms, while areas under Types I and III are shielded from these conditions [32]. The seasonal northeasterly monsoon enhances rainfall in the Eastern part of the Philippines due to orographic lifting [17]. So, Types II and IV have relatively wetter seasons than Types I and III [33]. LST can cool or warm faster and is more variable than T_{air} . This is a result of the complexity of surface types and variations in topography [6]. The difference between LST and T_{air} is associated with soil wetness and cloud amount [24]. Since Types I and IV climates receive higher amounts of rainfall because of their exposure to monsoons and trade winds, these conditions create a large difference between LST and T_{air} , resulting in a lower correlation. This is in line with the study of Pullen et al. [17] which stated that the closer the area is to the Pacific ocean, the greater the rate of change in the LST. Thus, any small variation in the LST or T_{air} in Type II and IV due to trade winds and monsoons could have resulted in the difference in the correlation value.

It was also observed that the LST- T_{air} relationship differences between climate types are more prominent at night relative to the day. For instance, the correlation range for the day is 0.47 to 0.68 while the night has a larger range of 0.39 to 0.81. The coupling of LST and T_{air} during the day is mainly influenced by the dynamic inputs of solar radiation [25]. This includes the effects of solar insolation, solar angle, surface shading, and advection, with cloud cover and microtopography also affecting this relationship. Contrary to this, as the sun is not present during the night, the LST- T_{air} difference variation is mostly influenced by emissivity properties of the surface, relative humidity, and wind speed [27]. This suggests that the effect of climate due to trade winds and monsoons will be much more notable during the night.

Limitations. Only areas that have weather stations that are operated by PAGASA were used in this study. Moreover, most of the areas that were excluded in this study are due to a large portion of missing LST data. With these, the descriptive power of Pearson's R might have been limited. Additionally, factors such as land cover, elevation, surface albedo, and solar insolation were the factors that might have affected the relationship but were not taken into consideration. Moreover, as multiple imputation was used to fill in the missing data and due to its nature, the researchers' data might have slight deviations

from the data of those with similar studies. Lastly, the standard deviation being greater than the mean is possible in some cases, and in this study, it can be attributable to the missingness of or error in the data.

Conclusion. - After assessing the relationship between LST and T_{air} under the different climatic types in the Philippines from 2005 to 2019, the results show that during the day, all climate types exhibited a positive relationship and moderate correlation. The same positive relationship can be observed during nighttime, however, the correlation varies. In Type I, it exhibited a strong correlation, meanwhile, Type II had a weak correlation. Lastly, both Types III and IV had a moderate correlation. Moreover, it has been observed that the strength of the correlation decreases as the locations approach the east or the Pacific ocean. Thus, this indicates that the LST and T_{air} relationship varies across climate types and factors such as geographical location, monsoons, and trade winds might have affected the relationship. Hence, this study is beneficial in understanding the dynamics of the LST and T_{air} relationship across the different climatic types in the Philippines. Moreover, this paper could also be used as a consideration in creating estimation models for the country's LST and T_{air} relationship.

Recommendations. - It is recommended that further studies should include more areas for a more accurate description of the relationship between LST and T_{air} across the different climate types. The relationship should also be assessed on daily and monthly data. In addition, the variation across the wet and dry seasons should also be investigated. Next, other methods for handling missing data should also be explored due to the large proportion of missing meteorological data. Moreover, the use of data from other meteorological stations that have a larger scope and more synoptic stations is recommended. Lastly, further studies should explore the comparison and quantification of the variation of LST and T_{air} in areas in the Philippines in terms of land cover, surface albedo, and other factors that might affect the relationship.

Acknowledgment. - The researchers would like to thank the Philippine Atmospheric, Geophysical, and Astronomical Services Administration (PAGASA) and the National Aeronautics and Space Administration's Land Processes Distributed Active Archive Center (LP DAAC) for providing them with the T_{air} data and LST data, respectively.

References

- [1] Krayenhoff ES, Voogt JA. 2010. Impacts of urban albedo increase on local air temperature at daily-annual time scales: model results and synthesis of previous work. *J Appl Meteorol Climatol.* 49:1634-1648. doi:10.1175/2010JAMC2356.1
- [2] Ibrahim GRF. 2017. Urban land use land cover changes and their effect on land surface temperature: case study using Dohuk City in the Kurdistan Region of Iraq. *Clim.* 5(1): 13. doi:10.3390/cli5010013
- [3] Schwarz N, Schlink U, Franck U, Großmann K. (2012). Relationship of land surface and air temperatures and its implications for quantifying urban heat island indicators—An application for the city of Leipzig (Germany). *Ecol Indic.* 18(2018), 693-704. doi:10.1016/j.ecolind.2012.01.001
- [4] Cao J, Zhou W, Zheng Z, Ren T, Wang W. 2020. Within-city spatial and temporal heterogeneity of air temperature and its relationship with land surface temperature. *Landsc Urban Plan.* 103979. doi:10.1016/j.landurbplan.2020.103979
- [5] Ali, JM, Marsh, SH, Smith, MJ. 2017. A comparison between London and Baghdad surface urban heat islands and possible engineering mitigation solutions. *Sustain Cities Soc.* 29(2017): 159-168. doi:10.1016/j.scs.2016.12.010
- [6] Tomlinson CJ, Chapman L, Thornes JE, Baker C. 2011. Remote sensing land surface temperature for meteorology and climatology: a review. *Meteorol Appl.* 18(3):296-306. doi:10.1002/met.287
- [7] Nichol JE, Fung WY, Lam K-se, Wong MS. 2009. Urban heat island diagnosis using ASTER satellite images and 'in situ' air temperature. *Atmos Res.* 94:276-284. doi:10.1016/j.atmosres.2009.06.011
- [8] Good EJ, Ghent DJ, Bulgin CE, Remedios JJ. 2017. A spatiotemporal analysis of the relationship between near-surface air temperature and satellite land surface temperatures using 17 years of data from the ATSR series. *J Geophys Res Atmos.* 122(17): 9185-9210. doi:10.1002/2017JD026880
- [9] Zhang P, Bounoua L, Imhoff ML, Wolfe RE, Thome K. 2014. Comparison of MODIS land surface temperature and air temperature over the continental USA meteorological stations. *Can J Remote Sens.* 40(2): 110-122. doi:10.1080/07038992.2014.935934
- [10] Philippine Institute for Development Studies. 2005. Basics on Philippine climatology. Economic Issue of the Day. <https://bit.ly/3InB7bN>
- [11] National Centers for Environmental Information (NCEI). NOAA's updated U.S. Climate Data will establish "New normal". 2021 Jun 8. [accessed 2021 Sept 14]. <https://bit.ly/3yBcJki>
- [12] Burgette LF, Reiter JP. 2010. Multiple imputation for missing data via sequential regression trees. *Am J Epidemiol.* 172(9):1070-1076. doi: 10.1093/aje/kwq260
- [13] Chhabra, Geeta. 2017. A Comparison of multiple imputation methods for data with missing values. *Indian J Sci Technol.* 10(19): 1-7. doi: 10.17485/ijst/2017/v10i19/110646
- [14] Cohen J. 1988. Statistical power analysis for the behavioral sciences (2nd ed.). Hillsdale, NJ: Lawrence Erlbaum Associates. doi:10.4324/9780203771587

- [15] Shen S and Leptoukh GG. 2011. Estimation of surface air temperature over central and eastern Eurasia from MODIS land surface temperature. *Environ Res Lett.* 6(4): 045206. doi:10.1088/1748-9326/6/4/045206
- [16] Vancutsem C, Ceccato P, Dinku T, and Connor SJ. 2010. Evaluation of MODIS land surface temperature data to estimate air temperature in different ecosystems over Africa. *Remote Sens Environ.* 114(2): 449–465. doi:10.1016/j.rse.2009.10.002
- [17] Pullen J, Gordon A, Flatau M, Doyle J, Villanoy C, Cabrera O. 2015. Multiscale influences on extreme winter rainfall in the Philippines. *J Geophys Res Atmos* 120: 3292–3309. doi:10.1002/2014JD022645
- [18] Chapin FS III, Randerson JT, McGuire AD, Foley JA, and Field CB. 2008. Changing feedbacks in the climate-biosphere system. *Front Ecol Environ.* 6(6): 313–320. doi:10.1890/080005
- [19] Guha S and Govil H. 2020. Land surface temperature and normalized difference vegetation index relationship: a seasonal study on a tropical city. *SN Appl Sci.* 2(10). doi:10.1007/s42452-020-03458-8
- [20] Anderson RG, Canadell JG, Randerson JT, Jackson RB, Hungate BA, Baldocchi DD, Ban-Weiss GA, Bonan GB, Caldeira K, and Cao L. 2010. Biophysical considerations in forestry for climate protection. *Front Ecol Environ.* 9(3): 174–182. doi:10.1890/090179
- [21] Sun Z, Wang Q, Batkhisig O, and Ouyang Z. 2015. Relationship between evapotranspiration and land surface temperature under energy-and water-limited conditions in dry and cold climates. *Adv Meteorol.* 2016(2016). doi:10.1155/2016/1835487
- [22] Lian X, Zhenzhong Z, Yitong Y, Shushi P, Kaicun W, Shilong P. 2017. Spatiotemporal variations in the difference between satellite-observed daily maximum land surface temperature and station-based daily maximum near-surface air temperature. *J Geo Res Atmos.* 122(4): 2254–2268. doi:10.1002/2016JD025366
- [23] Lambin E and Ehrlich D. 1996. The surface temperature-vegetation index space for land cover and land-cover change analysis. *Int J Remote Sens.* 17(3): 463–487. doi:10.1080/01431169608949021
- [24] Mutiibwa D, Strachan S, Albright T. 2015. Land surface temperature and surface air temperature in complex terrain. *IEEE J Sel Top Appl Earth Obs Remote Sens.* 8(10): 4762–4774. doi:10.1109/JSTARS.2015.2468594
- [25] Davy R, Esau I. (2016) Differences in the efficacy of climate forcings explained by variations in atmospheric boundary layer depth. *Nat Commun.* 7(11690): 1–8. <https://doi.org/10.1038/ncomms11690>
- [26] Hachem S, Duguay C, and Allard M. 2012. Comparison of MODIS-derived land surface temperatures with ground surface and air temperature measurements in continuous permafrost terrain. *Cryosphere.* 6(1): 51–69. doi:10.5194/tc-6-51-2012
- [27] Mildrexler D, Zhao M, Running S. 2011. A global comparison between station air temperatures and MODIS land surface temperatures reveals the cooling role of forests. *J Geophys Res.* 116: 1–15. doi:10.1029/2010JG001486
- [28] Mueller RW. (2013). Solar irradiance, global distribution. *J Sol. Energy.* 553–583. doi:10.1007/978-1-4614-5806-7_447
- [29] Lin S, Moore NJ, Messina JP, DeVisser MH, and Wu J. 2012. Evaluation of estimating daily maximum and minimum air temperature with MODIS data in east Africa. *Int J Appl Earth Obs Geoinf.* 18: 128–140. doi:10.1016/j.jag.2012.01.004
- [30] Chandler DL. 2010. Explained: Radiative Forcing. Massachusetts Institute of Technology. <https://bit.ly/3NKernE>
- [31] Colombi A, De Michele C, Pepe M, and Rampini A. 2007. Estimation of daily mean air temperature from MODIS LST in Alpine Areas. *EARSel eProceedings.* <https://bit.ly/3zrxik3>
- [32] Philippine Institute for Development Studies. 2005. Basics on Philippine climatology. *Economic Issue of the Day.* <https://bit.ly/3InB7bN>
- [33] Corporal-Lodangco I, Leslie L. 2017. Defining Philippine climate zones using surface and high-resolution satellite data. *Pro Comp Sci.* 114(2017): 324–332. doi:10.1016/j.procs.2017.09.068